THE JOURNAL OF PHYSICAL CHEMISTRY C
A JOURNAL OF THE AMERICAN CHEMICAL SOCIETY

pubs.acs.org/JPCC

Article

Fluorescent Probe of Aminopolymer Mobility in Bulk and in Nanoconfined Direct Air CO_2 Capture Supports

Helen Correll, Noemi Leick, Rachel E. Mow, Glory A. Russell-Parks, Simon H. Pang, Thomas Gennett, and Wade A. Braunecker*

Cite This: *J. Phys. Chem. C* 2022, 126, 10419−10428

Read Online

ACCESS | Metrics & More | Article Recommendations | Supporting Information

ABSTRACT: Poly(ethylenimine) (PEI) is widely recognized as an efficient carbon capture medium. When loaded onto mesoporous oxide supports, the polymer becomes particularly attractive for direct air capture (DAC) applications given the high surface area of the composites, the low volatility of the polymer, and the excellent cyclability of the system. As polymer segmental mobility is coupled with CO_2 uptake and diffusion, understanding how that mobility is influenced by nanoconfinement will ultimately be critical to the development of more efficient DAC systems. Here, we discuss our development of a fluorescent probe molecule based on tetrakis(4-hydroxyphenyl)ethylene. As the fluorescence intensity of this molecule and the shape of the emission spectra are strongly dependent on the viscosity of the supporting medium, doping PEI-composites with this fluorescent probe can provide sensitive indication of polymer glass transition and/or melting temperatures across a wide range of temperatures (−100 to +100 °C). Herein, we demonstrate how this molecule can be used as a ratiometric probe to study bulk PEI dynamics and confinement effects in mesoporous silica as influenced by pore functionality, polymer fill fraction, and polymer architecture.

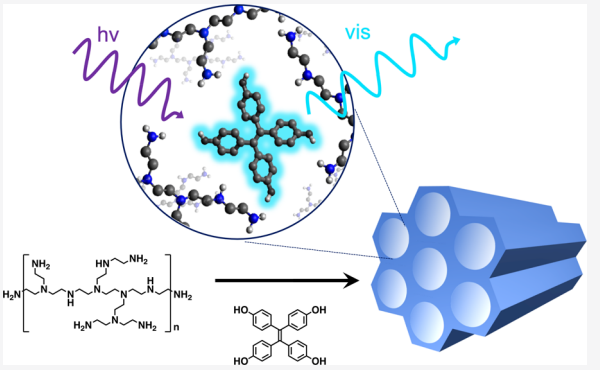

1. INTRODUCTION

As countries around the world work to reduce their carbon footprint, numerous reports[1,2] and reviews[3−5] anticipate that direct air capture (DAC) systems will play an increasingly important role in curbing net global greenhouse gas emissions through CO_2 removal. Among the different types of capture systems being studied for DAC,[6] chemisorbent amines, such as poly(ethylenimine) (PEI) supported in solid mesoporous oxide composites, are receiving extensive attention.[7−17] In addition to having CO_2 adsorption enthalpies in an ideal range to perform separations at the low partial pressure of CO_2 in air,[18] the low volatility, commercial availability, and high cyclability of PEI in combination with the high surface area of the support leave these composites well suited for DAC applications.

Understanding aminopolymer mobility plays an important, but often overlooked, role in the optimization of these DAC systems. In general, gas diffusion through any polymeric material is coupled with polymer segmental mobility. Rubbery polymers, or polymers that are employed above their glass transition temperature (T_g), are able to promote more efficient gas diffusion than glassy polymers.[19] Thus, aminopolymers with a low T_g/high mobility are attractive for promoting efficient gas diffusion in DAC. However, their segmental mobility is also dramatically influenced by the dynamic uptake and release of CO_2 upon cycling, as electrostatic cross-links develop throughout the polymer when amine and CO_2 react to produce carbamate species. This phenomenon significantly rigidifies the aminopolymer and can in turn create a barrier for subsequent gas diffusion.[20] For this reason, inert plasticizers and additives such as poly(ethylene glycol) (PEG)[20] have been blended with aminopolymers in an effort to decrease their rigidity and promote more optimal uptake kinetics. Additionally, polymer mobility can be influenced by a variety of surface, interface, and confinement effects[21−23] that vary quite dramatically from the bulk when loaded into nanocomposites. For example, the thermal transitions of PEG loaded into various framework supports can shift by as much as 100 °C due to different polymer−support interactions.[24] Given the myriad factors that can influence the mobility of aminopolymers and polymeric additives in DAC, the design of more efficient DAC processes would benefit from a thorough fundamental understanding of mobility.

Received: February 15, 2022
Revised: May 28, 2022
Published: June 14, 2022

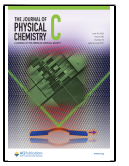

https://doi.org/10.1021/acs.jpcc.2c01099
J. Phys. Chem. C 2022, 126, 10419−10428

Conventional techniques for probing generic thermal transitions and mobility of bulk polymers include viscometry, thermal or dynamic mechanical analysis (DMA), and differential scanning calorimetry (DSC). However, these techniques are often either not sensitive enough to determine transitions in thin films or at low polymer loadings in composites or they are of limited application for probing polymer properties within nanoconfined pores. Several specialized techniques have been developed to study the mechanical properties of ultrathin films, including so-called bubble inflation and buckling measurements, which have been used to characterize unique behavior induced by substrate interactions, including glassy softening[25,26] and rubbery stiffening.[27,28] Broadband dielectric spectroscopy was recently used in conjunction with NMR[29] to infer information about the mobility of specific regions of PEI under different conditions, *i.e.*, backbone, side chain, and chain end mobility in the bulk *vs* in confined composites. Neutron scattering has also been employed to provide particularly rich information about the nature of PEI mobility within different mesoporous composites as a function of polymer loading and pore functionality.[30−32] However, given the vast number of parameters that can influence aminopolymer mobility in DAC systems, the development of sensitive benchtop techniques that can provide additional or complementary information to the aforementioned methods concerning mobility in nanoconfinement would be of significant value for advancing the field.

The recent development of several fluorescence techniques for characterizing glass-forming polymers[33] offers some intriguing opportunities for evaluating DAC-based systems. While fluorescence can be used to characterize the T_g of bulk polymers,[34,35] the sensitivity of this benchtop technique and its ability to provide location-specific information through the tethering of probe molecules make fluorescence particularly powerful for studying polymer properties at the nanoscale. In addition to studying glass transitions, fluorescence measurements can also aid in the physical characterization of polymeric properties such as mobility and diffusion,[36,37] physical aging,[38,39] and mechanical response.[40,41] These measurements can further be utilized to study the effects of complex geometries, including capped films,[23] multilayer films,[39,42] polymer−polymer interfaces,[43,44] and nanocomposites.[23,45] While fluorescent probes have also been tethered to PEI[46] and to the walls of mesoporous silicas[47] for various applications, to our knowledge, there are no reports on the use and development of a fluorescent probe designed specifically to study PEI thermal transitions, much less in nanoconfined systems employed in DAC.

Herein, we report our efforts to develop such a probe whereby we identified a suitable fluorogen compatible with PEI and benchmarked its response in different environments across a wide swath of temperatures. We then studied fluorescence in a series of PEI samples with different molecular weights and architectures and probed relative PEI mobility in confined mesoporous silicas as a function of different polymer loadings and pore functionalities. The results were then verified through a comparison with literature studies using other techniques to probe PEI dynamics.

2. EXPERIMENTAL SECTION

2.1. Materials. Tetraphenylethylene (TPE) derivatives were purchased from TCI. 2,6-Dimethylbenzonitrile (DMB) was purchased from Fischer Scientific. All other reagents, chemicals, and polymers were purchased from Aldrich and used without purification, unless otherwise noted. SBA15-OH[30] and SBA15-CH_3[31] were synthesized according to literature procedures.

2.2. Fluorescent Doping Procedure. Bulk polymers and small molecules were doped with tetrakis(4-hydroxyphenyl)-ethylene (THPE) (0.02−1 wt %) by stirring the mixtures under a N_2 atmosphere in the dark well above the mp/glass transition temperature of a given matrix (*e.g.*, 50 °C for branched PEI, 100 °C for linear PEI). Composites were prepared by first stirring pre-doped PEI and SBA15 in separate methanol solutions (∼10 mg/mL) for 1 h and then combining and further stirring for 3 h. The combined mixture was then placed on a rotary evaporator to remove the methanol. Final degassing was performed on a Schlenk line under vacuum (∼100 mTorr) at 110 °C for 48 h in the dark to remove any CO_2, moisture, and residual solvent. Samples were left under vacuum and taken directly into an inert atmosphere for further handling.

2.3. Differential Scanning Calorimeter (DSC). The phase changes of the samples were compared with data obtained from a TA Instruments DSC 25 equipped with a Discovery liquid N_2 pump allowing a minimum sampling temperature of −150 °C. Samples were prepared under an inert He atmosphere. The system was calibrated at the temperature ramp of choice using an indium reference sample prior to the measurements. The samples were heated at a 10 °C/min ramp rate with a 50 mL/min N_2 flow through the cell and a 307 mL/min base purge.

2.4. Isotherms. N_2 physisorption isotherms at 77 K performed in a Micromeritics TriStar 3020 were collected with 45 s equilibration time in the p/p_0 range of 0−0.001, which was decreased to 10 s for $p/p_0 > 0.001$. From these isotherms, the specific surface area and pore volume of the samples were extracted through the Brunauer−Emmett−Teller (BET) in the range of p/p_0 from 0.05 to 0.2 and the Barrett−Joyner−Halenda (BJH) method from the total N_2 adsorbed at p/p_0 0.95, respectively.

2.5. Thermogravimetric Analysis (TGA). PEI content in the composites was estimated using a TA Instrument Q600 TGA apparatus and a literature procedure.[48] Weight loss from 120 to 900 °C under a 100 mL/min flow of N_2 diluted air was recorded at 10 °C/min and normalized by the residual mass at 900 °C.

2.6. Photoluminescence (PL) Spectroscopy. PL experiments were conducted on a custom-built Princeton Instruments spectrometer using a liquid N_2-cooled Si CCD (PyLoN) array for collecting visible−near-infrared (NIR) spectra (400−900 nm). Intensity calibration was performed daily using an IntelliCal USB-LSVN (9000-410) calibration lamp. Samples were placed in a 2 mm quartz cuvette and excited with a 365 nm light-emitting diode (LED) (7.5 nm full width at half-maximum (FWHM)). A 400 nm longpass filter was employed between the sample and collection fiber. Emission spectra were collected from 200 to 800 nm using a 150 g/mm grating with an 800 nm blaze and a 3 mm slit; 20 spectra were averaged with an overall exposure time of ∼5 s. Temperature control was achieved with an Oxford Instruments OptistatDN sample-in-N_2-vapor cryostat. Unless otherwise specified, polymer samples were both cooled and heated at a rate of ∼1 °C/min. The standard error was calculated by dividing the standard deviation by the square root of the sample size, typically attained from three different independent samples.

https://doi.org/10.1021/acs.jpcc.2c01099
J. Phys. Chem. C 2022, 126, 10419−10428

3. RESULTS AND DISCUSSION

3.1. Tetraphenylethylene Derivatives as Ratiometric Fluorescent Probes. A wide variety of fluorescent probe molecules and techniques have recently been employed to study diffusion and mobility phenomena in polymer systems.[33] Among these probe techniques, aggregation-induced emission luminogens (AIEgens) are particularly sensitive to minute changes in the viscosity of their supporting matrix. AIEgens have high photoluminescent quantum yield (PLQY) when aggregated or suspended in a frozen or glassy matrix, but PLQY decreases substantially when dissolved in a fluid system.[49] Tetraphenylethylene (TPE) is an archetypal AIEgen whose derivatives have been widely used for sensing applications ranging from biomolecular science[50,51] to mechanoresponsive systems.[52] The viscosity-dependent PLQY of TPE has also recently been employed to study glass transition dynamics of amorphous polymer films.[35,53]

The fluorescence of TPE is largely governed by intramolecular rotations.[49] In a fluid matrix, rotation of the phenyl groups around their single bond axes in photoexcited TPE molecules contributes to nonradiative decay from their photoexcited state. Furthermore, the central olefinic double bond of TPE can open in the photoexcited state, leading to torsional rotation around the central C−C bond that creates significant additional friction with solvating molecules and subsequent thermal relaxation. Hence, TPE becomes virtually nonemissive when well solvated in low or nonviscous fluids. The shape of the TPE emission spectra can also be highly dependent on the viscosity of the supporting matrix, emitting a photon of one wavelength when rotational motion is restricted, but emitting at a longer wavelength when the excited state molecule can rotate into a more energetically favorable conformation with a smaller highest occupied molecular orbital (HOMO)−lowest unoccupied molecular orbital (LUMO) transition.[54] The dependence of the shape of the emission spectrum on viscosity affords an opportunity to employ TPE derivatives as ratiometric fluorescent probes, whereby the ratios of intensities at two or more wavelengths are recorded. In this way, the technique is effectively self-referencing and allows for the comparison of samples with different geometries, light-scattering properties, concentrations of the fluorescent probe, and even loss of fluorescence intensity with time due to photobleaching.[55]

In principle, TPE derivatives can be introduced into a polymer matrix to probe mobility via several different strategies, each with its own nuanced advantages. If the probe molecule has good miscibility with the matrix over the full range of temperatures being studied, it has been demonstrated that simply doping the probe into the system can provide a reliable indicator of polymer T_g.[35] When miscibility/solubility is a concern, TPE derivatives can also be covalently tethered to aminopolymers.[35,46] For nanocomposite systems (*i.e.*, mesoporous silica impregnated with aminopolymer), TPE can also in principle be tethered to the pore wall.[47] While we found that TPE itself is not soluble in branched PEI, the commercially available analogue tetrakis(4-hydroxyphenyl)ethylene (THPE) could be well dispersed in bulk aminopolymers (Figure 1). We thus opted to first consider simple doping strategies in this initial fluorescence investigation of PEI mobility.

3.2. Tetrakis(4-hydroxyphenyl)ethylene (THPE) Fluorescence in Small-Molecule Matrices. As discussed, even aminopolymers with very low glass transition temperatures can effectively become glassy at higher temperatures upon CO_2 uptake; thus, a fluorescent probe developed to study mobility in aminopolymer-based DAC systems would ideally operate in a predictable fashion over a wide range of temperatures. Here, we begin to benchmark the fluorescence response of THPE in several different small-molecule organic solvents, namely, tetrahydrofuran (THF), naphthalene, and 2,6-dimethylbenzonitrile (DMB), with corresponding mp values of −109, 80, and 89 °C, respectively. Small-molecule matrices were attractive for this initial study because they tend to have well-defined thermal transitions as well as tunable melting point (mp) values and polarities.

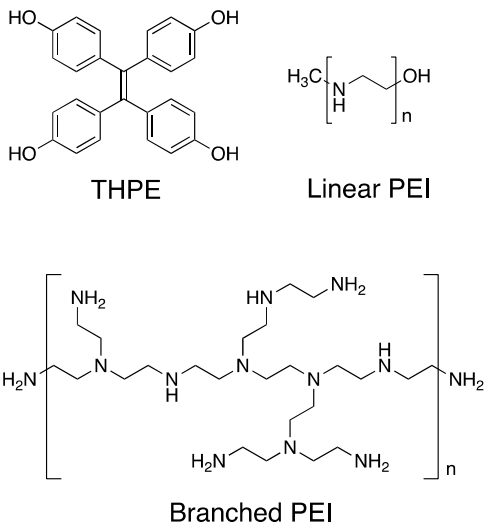

Figure 1. Chemical structures of tetrakis(4-hydroxyphenyl)ethylene (THPE) as well as linear and branched poly(ethylenimine) (PEI) are used in this work.

While THPE is essentially nonemissive in THF at room temperature (rt), the fluorescence spectrum of a 0.02 wt % solution of THPE in frozen THF at −180 °C showed intense emission at a λ_{max} of 458 nm (Figure 2, top panel). This observation agrees well with previous reports citing an emission λ_{max} near 450 nm, depending on the nature of the solid-state matrix.[56] Both the emission λ_{max} and PLQY stayed essentially constant between −180 and −140 °C, changing less than 2%. However, between −120 and −100 °C, the relative fluorescence intensity dropped by a factor of 20 (Figure 2, middle panel), and λ_{max} red-shifted with increasing temperature. Above −100 °C, λ_{max} stayed essentially constant at ∼525 nm, though the signal-to-noise ratio became very poor under these conditions. Overall, the results are highly consistent with the behavior of TPE in 3-methylpentane,[54] which similarly displayed three temperature-dependent "regions" with differing fluorescence responses and emission λ_{max} shifting from 460 to 525 nm. In the lower panel of Figure 2, we plot the change in ratiometric intensity as a function of temperature; 530 and 460 nm were selected as representative of λ_{max} at the relatively warm and cold temperatures, respectively, for the different samples studied throughout this manuscript. From the plots in Figure 2, both fluorescence intensity at 460 nm and the change in ratiometric intensity appear to be good indicators of the mp of THF (−109 °C).

The same general trend in fluorescence behavior of THPE was observed for a 0.02 wt % sample doped into DMB, albeit shifted at 200 °C. This sample was prepared by stirring THPE

https://doi.org/10.1021/acs.jpcc.2c01099
J. Phys. Chem. C 2022, 126, 10419−10428

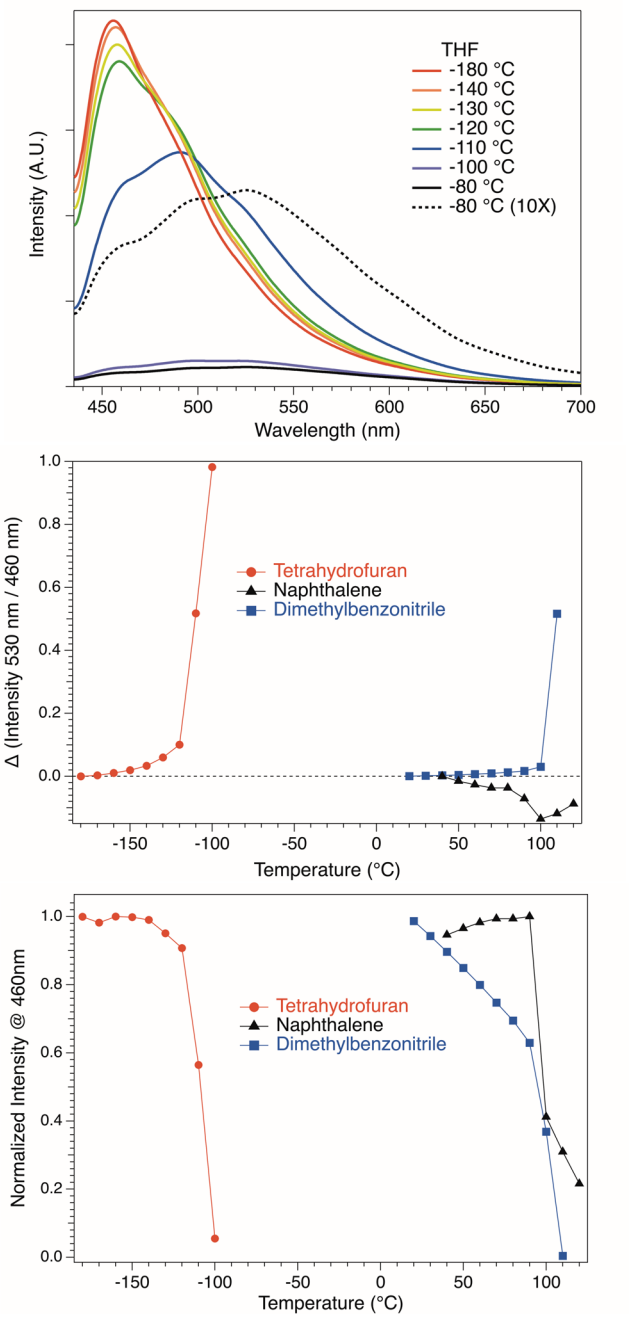

Figure 2. (Top) Emission spectra of tetrahydrofuran doped with 0.02 wt % THPE as it is heated through its melting point at −109 °C. Excitation at 365 nm. (Middle) Normalized fluorescence intensity at 460 nm as a function of temperature for 0.02 wt % THPE solutions in tetrahydrofuran (red circles), naphthalene (black triangles), and 2,6-dimethylbenzonitrile (blue squares). (Bottom) Ratiometric fluorescence intensity (530/460 nm) for the same data set. Dashed vertical lines indicate literature mp values.

and DMB at 110 °C for 1 h under a N_2 atmosphere in the dark and then cooling to rt. The ratiometric fluorescence intensity (530/460 nm) of this sample remained relatively constant between 20 and 80 °C but then undergoes dramatic change above the mp of DMB (89 °C). While the fluorescence intensity at 460 nm drops ∼30% between 20 and 80 °C, there is a marked decrease above the mp of DMB, and the solution was only weakly emissive above 110 °C.

In contrast to the THF and DMB solutions, the ratiometric fluorescence response of THPE was markedly different when the molecule was dispersed into a matrix where it was poorly miscible, such as naphthalene. While THPE would fully dissolve in the former two solutions, rapid stirring in liquid naphthalene at 110 °C for 1 h produced a very fine suspension that scattered light, indicative of THPE aggregation. Upon heating a 0.02 wt % suspension from rt through its mp (80 °C) up to 120 °C, the emission maximum remained essentially constant near 450 nm, and no dramatic increase in ratiometric intensity near the mp of the solvent was observed as in the other two solvents. The results were consistent with our observation that THPE aggregates in liquid naphthalene, which would restrict intramolecular rotation, even above the melting temperature of the matrix. We note that while the shape of the emission spectra does not change, the absolute fluorescence intensity of THPE in naphthalene does start to drop significantly above 90 °C (Figure 2, middle panel); taken as a whole, the results suggest that THPE can be employed as a reliable indicator of small-molecule phase changes over a range of nearly 200 °C, and furthermore, the molecule is an excellent ratiometric probe over this range when well solvated in its matrix (THF and DMB).

3.3. Polymer Mobility and Thermal Transitions.

3.3.1. DSC Data. Prior to investigating polymer thermal transitions with our fluorescent probe, we first used DSC to determine the effect of doping up to 1 wt % of the probe molecule into a series of PEI samples with different molecular weights and architectures. A fundamental requirement of using any probe molecule to investigate the mobility of a medium is that the presence of the probe should have a minimal effect on the medium. In Table 1, thermal transitions of the bulk

Table 1. Thermal Transitions Recorded with DSC (°C)[a]

polymer	neat	1 wt % TPHE
L-PEI 2500[b]	54	53
B-PEI 800[c]	−65	−64
B-PEI 25,000[c]	−52	−50

[a]Heating rate = 10 °C/min. [b]Onset temperature of melting (°C). [c]Estimation of the polymer glass transition temperature (°C).

polymer recorded by DSC are compared with fluorogen-doped polymer transitions for branched PEI samples with weight average molecular weights (M_w) of 800 and 25,000 g/mol and a linear PEI sample with M_w ∼ 2500 g/mol. The traces are illustrated in Figure S3 and were recorded at a heating rate of 10 °C/min. Values of T_g for the branched PEI samples were estimated at −65 and −52 °C for low- and high-molecular-weight samples, respectively. The onset of T_m for the linear PEI sample occurred at 54 °C. The values for both the branched[57] and linear[58] samples were fully consistent with literature values that employed the same heating rates. As seen in Table 1, fluorogen-doped polymer samples differed by only 1−2 °C when compared with the neat sample. Although doping at lower concentrations of a fluorogen (0.02 wt %) made these already small differences completely negligible, employing a 1 wt % fluorogen gave a substantially better signal-to-noise ratio during fluorescence measurements with polymer systems. An improved signal-to-noise ratio allowed spectra to be collected with an overall lower intensity of excitation light and/or with a shorter duration of light exposure, both of which lead to less artifacts in the mobility data (*vide infra*).

https://doi.org/10.1021/acs.jpcc.2c01099
J. Phys. Chem. C 2022, 126, 10419−10428

3.3.2. Photostability and Cycling. In the presence of oxygen, TPE and its derivatives can be photo-oxidized to a diphenylphenanthrene derivative within minutes of UV exposure at irradiances used in this work (~1 mW/cm^2), both in solution and in the solid state.[59] However, under an inert N_2 atmosphere, we observed THPE to generally be photostable toward any degradation on the timescale of our experiments. We performed a photostability study on a 40 wt % composite of branched PEI 800 and commercial grade mesoporous silica (MCM-41). The latter parent compound had a surface area of ~1020 m^2/g, an average pore-size distribution of 2.5 nm, and a pore volume of 0.8 cm^3/g. PEI was doped with 1 wt % THPE relative to the polymer. The stability of the probe was then investigated over a wide range of temperatures (−120 to 100 °C) by holding the sample at a given temperature under an inert atmosphere, exciting the sample for 5 s at ~1 mW/cm^2 of 365 nm light to collect an emission spectrum, and then performing four subsequent measurements over the course of 10 min. Emission spectra from each of these five measurements were compared and monitored for changes due to photobleaching or degradation. We found that below rt, the first and fifth emission spectra were virtually indistinguishable, implying excellent photostability under these conditions. At rt, the intensity of the first and fifth emission spectra varied only 1%. At 100 °C, the intensity of the fifth emission spectra was ~5% lower than that of the first spectrum, though the ratiometric intensity (530/460 nm) remained essentially constant. The results suggest that the probe is more than sufficiently photostable during the collection of a typical emission spectrum to infer reliable mobility information at all temperatures employed in this manuscript.

We note that at temperatures above the T_g of the polymer, where both the polymer matrix and the THPE molecule are more mobile, longer durations of light excitation/exposure (on the order of minutes) can result in a red shift in the recorded emission spectrum as compared to a spectrum collected over 5 s. Presumably, this is the result of localized heating that can be attributed to the excited state THPE molecule rotating more freely and dissipating more energy to the matrix through nonradiative (thermal) decay mechanisms. If allowed to re-equilibrate for several minutes after longer light exposures, the spectrum will blue-shift back to its original shape. We note this as a word of caution when inferring differences in polymer mobility across samples at a given temperature; we found it is critical that light exposure is both minimized and held constant across samples. Below the polymer T_g where TPHE rotation is restricted, this reversible red−blue shift phenomenon was not observed.

We also cycled THPE-doped PEI above and below its T_g to ensure that THPE was not aggregating with time at colder temperatures and that the measurements were fully reproducible upon cycling. In Figure 3, ratiometric fluorescence intensity is illustrated for a 50 wt % composite of branched PEI 800 and mesoporous silica (SBA15-OH). PEI was doped with 1 wt % THPE and the sample was cycled six times above and below its T_g (−65 °C) for a total of 12 measurements. Figure 3 illustrates how constant the ratio remains at a given temperature, particularly for cycles 2−6. The subtle difference in ratiometric intensities between corresponding data points in cycles 1 and 2 is likely due to the uncontrolled thermal history of the first cycle (see the discussion in Section 3.3.3). Overall,

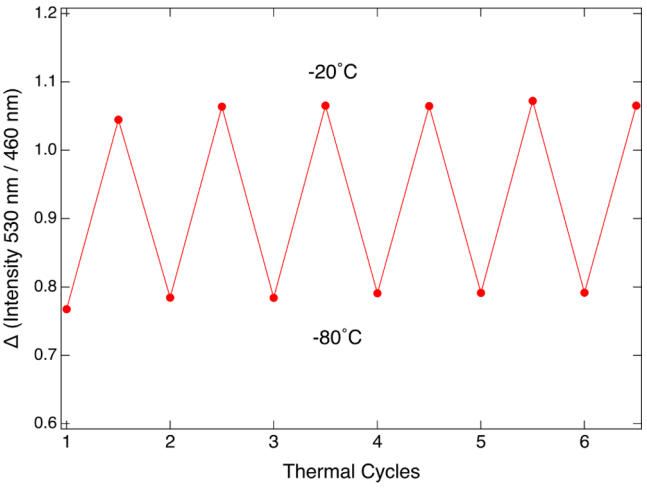

Figure 3. Ratiometric fluorescence intensity (530/460 nm) for SBA15-OH with 50 wt % PEI doped with 1 wt % THPE. The sample was cycled 6 times between −80 and −20 °C, above and below the T_g of −65 °C.

the cycling experiment provides additional evidence for the reliability and reproducibility of these measurements.

3.3.3. Thermal History. For most fluorescence measurements conducted in this manuscript, the intensity of the emission spectrum changes more than an order of magnitude across the temperatures investigated, dropping in intensity as the temperature is increased. As a high-fluorescence signal-to-noise ratio is typically achieved by optimizing several different light acquisition parameters for a given sample, it is desirable to optimize those parameters at the temperature where the signal is most intense so as not to risk saturating the detector midway through a series of temperature-dependent measurements with the increasing signal. For this reason, the fluorescence signal-to-noise ratio was optimized at low temperatures for most of our measurements, at which point it was pragmatic to collect spectra upon heating.

We acknowledge that measurements probing polymer mobility as a function of heating (vs cooling) are technically estimating the so-called fictive temperature of a material rather than the glass transition; the latter can only be attained upon cooling.[60] We provide several references here discussing the nuances of these parameters and perspectives on the kinetics of glass-forming polymers.[61−63] We note that it has also been proposed[64] and observed[60] that when the thermal history of a given sample is well controlled and rates of cooling and heating are equivalent, values of fictive and glass transition temperatures vary by only ~1 °C and are thus close approximations of each other. When the rates of heating and cooling are not equivalent, volumetric changes associated with thermal expansion are complicated by the kinetics of structural recovery. The phenomenology is, however, generally well understood.[62] For example, if cooling is relatively rapid, the polymer can be kinetically arrested far from its equilibrium state. A slow heating following rapid cooling can initially result in negative thermal expansion as arrested chains are effectively afforded more time to approach their equilibrium state at a given temperature.[60] Here, we study the fluorescence response of THPE-doped PEI as a function of thermal history to gauge the sensitivity of our technique in detecting and studying such phenomena.

https://doi.org/10.1021/acs.jpcc.2c01099
J. Phys. Chem. C 2022, 126, 10419−10428

In Figure 4, we illustrate the fluorescence response of two samples with different thermal histories. The first was cooled

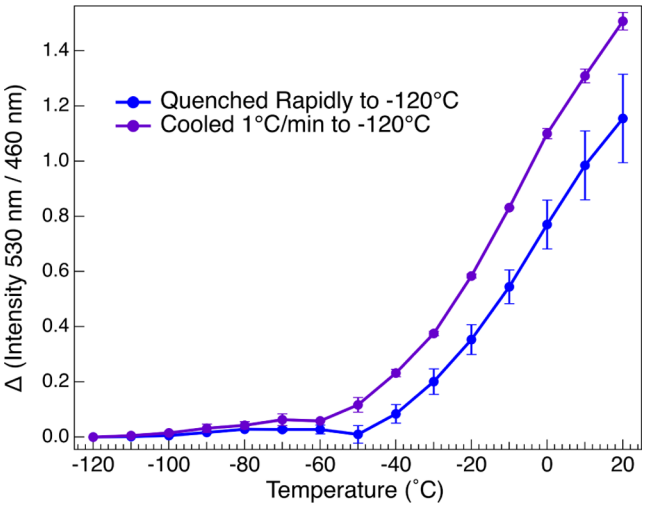

Figure 4. Temperature dependence of the ratiometric fluorescence intensity (530/460 nm) of bulk PEI 800 doped with 1 wt % TPHE upon heating at 1 °C/min. The cooling rate of one sample was controlled at 1 °C/min (purple), while the other sample (blue) was flash-cooled to −120 °C in 15 min.

slowly at 1 °C/min from 20 to −120 °C, while the second sample was quenched to −120 °C one order of magnitude more quickly (within ∼15 min). Emission spectra were then collected for both samples at a heating rate of 1 °C/min (representative spectra are illustrated in Figure S2). A comparison of the two data sets in Figure 4 reveals differences in the fluorescence response as a function of their cooling rate/thermal history. Those responses begin deviating from each other at approximately −70 °C (near T_g estimated from DSC). For the sample with equivalent rates of heating and cooling, the smooth increase in ratiometric fluorescence intensity is consistent with a general increase in mobility and/or thermal expansion of the polymer matrix. In contrast, we observed that the ratiometric response of the rapidly cooled sample initially decreased upon heating from −70 to −50 °C before increasing again at higher temperatures (see Figure 4). The results are consistent with literature examples of systems that experience negative thermal expansivity upon slow heating after rapid cooling.[60] In addition to illustrating the importance of controlling the thermal history of a sample, we believe that these results also highlight the power of the probe to detect and study sensitive changes in glass-forming kinetic phenomena, such as polymer fragility,[65] which we are currently evaluating.

3.3.4. PEI Molecular Weights and Architecture. The fluorescence responses of bulk linear PEI 2500 as well as branched PEI 800 and 25,000 doped with THPE are illustrated in Figure 5. The dashed lines on the plot indicate values of T_g and the onset of T_m estimated from DSC. As can be seen in this figure, there is a sharp transition in the ratiometric fluorescence response of THPE-doped linear PEI between 50 and 60 °C, which corresponds well to the onset of T_m determined by DSC as 53 °C for this sample (Table 1). The rapid change in fluorescence response is similar to that observed in the melt transitions of the small-molecule matrices discussed earlier. In the branched PEI samples, the ratiometric

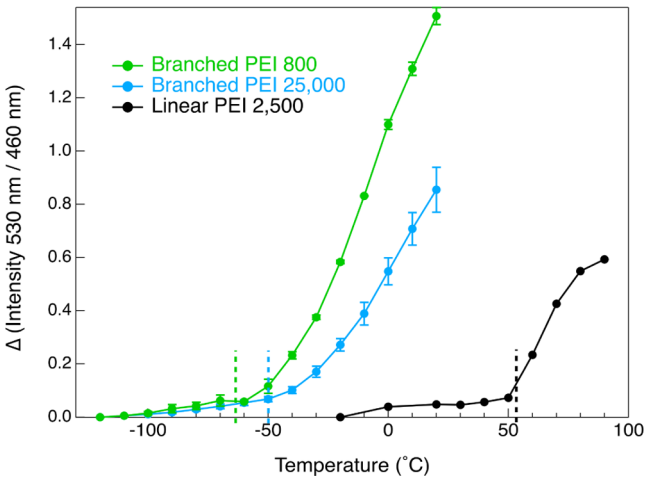

Figure 5. Temperature dependence of the ratiometric fluorescence intensity (530/460 nm) of branched PEI 800 (green), branched PEI 25,000 (blue), and linear PEI 2500 (black). Dashed lines illustrate T_g and onset of T_m estimated from DSC.

fluorescence response is also pronounced as the material passes through a glass transition; however, changes in fluorescence response are generally more gradual in these amorphous polymers than in systems that experience formal melting. The behavior can be rationalized by considering that glass transitions are pseudo-second-order transitions characterized by a change in the slope of a specific volume at T_g rather than a large stepwise change in specific volume at T_m (see Figure 3 in Burroughs et al.[33]).

We note that certain techniques (*e.g.*, dielectric spectroscopy) are sensitive to sub-T_g molecular motions. While the glass transition is generally believed to be associated with the coordinated motion of 50−100 carbon atoms (often labeled the α-relaxation),[66] dielectric spectroscopy has been used to identify independent movements in the side chains of PEI associated with 4−8 carbon atoms (a.k.a. β-relaxation) and terminal amino group motion (γ-relaxation) at temperatures well below T_g of branched PEI.[57] Both of these motions are believed to facilitate the physical aging phenomenon in polymers held below their T_g.[67] They have also been invoked to explain penetrant transport into glassy polymers, including diffusivity of CO_2 through glassy poly(vinyl acetate) as a function of polymer aging.[68] However, it does not appear from the data illustrated in Figure 5 collected down to −150 °C that sub-T_g molecular motions can be detected with this probe molecule. The results suggest that the probe is much more adept at detecting so-called α-relaxations than β- or γ-relaxations.

3.3.5. Mobility of PEI in Confinement. Having studied the fluorescence response of THPE in bulk polymer and small-molecule matrices, we turn now to investigate the probe response in more accurate models of DAC operating systems, namely, PEI loaded mesoporous oxide composites. Interactions between the polymer and support in these composite gas sorbents are well known to influence performance in these materials; *e.g.*, pore wall functionalization and polymer fill fraction have been correlated with CO_2 sorption kinetics and capacities.[30,31] Due to the well-defined and tunable nature of mesoporous silicas such as SBA15, aminopolymer-loaded SBA15 composites are often employed in both fundamental and applied systematic DAC studies.[3] Here, we probe the

https://doi.org/10.1021/acs.jpcc.2c01099
J. Phys. Chem. C 2022, 126, 10419−10428

mobility of PEI 800 in composites with native silanol-terminated silica (SBA15-OH) as well as hydrophobic-functionalized silica (SBA15-CH_3), where silanol functional groups are capped via reaction with hexamethyldisilazane. The effect of the polymer fill fraction in both composites is also investigated.

Details of the preparation of the fluorescent-doped composites are provided in the experimental section. The surface area and pore volumes of the parent materials and composites were characterized by nitrogen-physisorption isotherms, and the PEI content was determined via TGA. Nominal polymer fill fractions of 40 and 50 wt % were targeted for SBA15-CH_3 and SBA15-OH, respectively, as these values are near the theoretical loading limit for each composite. The 5 wt % composites were also used for each system for comparison to literature data concerning polymer mobility at specific fill fractions. Data characterizing these composites are summarized in Table 2. Pore-size distributions are illustrated in Figure S5.

Table 2. Characterization of PEI 800-Mesoporous Composites

sample	pore volume (cm^3/g)	organic content (wt %)[a]
SBA15-OH	0.99	4.3[b]
5 wt % PEI/SBA15-OH	0.75	11
50 wt % PEI/SBA15-OH	0.08	56
SBA15-CH_3	0.66	8.1
5 wt % PEI/SBA15-CH_3	0.64	12
40 wt % PEI/SBA15-CH_3	0.16	45

[a]Estimated from mass loss between 150 and 895 °C via TGA. [b]Partially attributed to decomposition of silanol surface groups.

Figure 6 illustrates the ratiometric fluorescence data measured for the SBA15 composites alongside bulk PEI. The data indicates that confinement of PEI in mesoporous silica in all cases significantly lowers its mobility relative to the bulk. A comparison of the fluorescence response for the two samples near their theoretical loading suggests that PEI in the SBA15-CH_3 composite has higher mobility than PEI in SBA15-OH. The results are consistent with previous literature investigations using quasielastic neutron scattering (QENS) and molecular dynamics (MD) simulations to establish the nature of polymer−support interactions and polymer chain dynamics.[31] Those studies determined that hydrophobic functionalization of silica weakens the silica−PEI interactions and results in greater mobility of the PEI than in composites where more extensive hydrogen bonding with silanol surface groups existed. Furthermore, the fluorescence data suggests that PEI in both 5 wt % samples is significantly less mobile than that in the higher fill fraction composites, which is also consistent with the literature QENS studies.

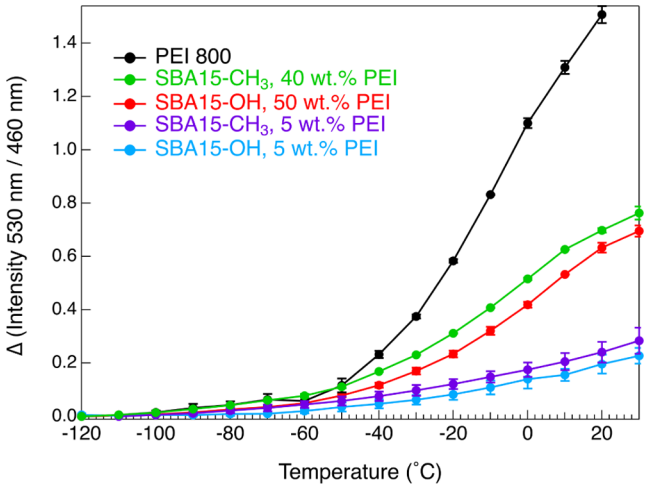

Figure 6. Temperature dependence of the ratiometric fluorescence intensity (530/460 nm) of bulk PEI 800 as well as mesoporous silica composites with different PEI 800 loadings and surface functional groups (−OH vs −CH_3).

To reduce or eliminate the possibility that THPE may migrate as a function of temperature in the composites and begin interacting with the pore walls, we synthesized a TPE-based probe that was covalently tethered to PEI. Details of the synthesis and characterization are recorded in the Supporting Information. In Figure S9, we compare the ratiometric fluorescence intensity of a composite where THPE was doped into the system vs a composite with tethered TPE. The fluorescence responses of these two systems are remarkably similar. The results provide additional support that the polymer mobility we believe we are probing is not an artifact of temperature-dependent probe migration.

Finally, we note that thermal transitions could be detected with DSC in all composites near their theoretical loading; a shift in PEI 800 T_g was recorded from −65 °C in the bulk to between −58 and −56 °C in confinement (Figure S4). However, no thermal transitions were detected for the 5 wt % composites. In the latter samples, a relatively high fraction of the material could be present both at the polymer−support and polymer−air interfaces. This can result in a large mobility gradient across the thin supported films that can be difficult to disentangle.[69,70] Indeed it has been argued that the field needs to look beyond simple T_g measurements to characterize the dynamics of thin supported polymer films.[71] As such, this fluorescence technique allows for powerful qualitative comparisons of relative mobilities across different samples over a range of temperatures that few other benchtop techniques can provide.

4. CONCLUSIONS

This work represents an effort to develop a suitable fluorescent probe for extracting information about aminopolymer chain dynamics in confinement that can otherwise be difficult to ascertain. After benchmarking the response of our probe in different bulk environments across a wide swath of temperatures, we determined the photo and cycling stability of the probe and established its ability to detect subtle polymer aging phenomena based on the thermal histories of the sample. We then demonstrated that these fluorescence measurements could be used to study chain dynamics across a series of PEI samples with different molecular weights and architectures. We further probed PEI chain dynamics in confined mesoporous silicas as a function of different polymer loadings and pore functionalities. The results highlight the power of the technique to detect subtle changes to polymer dynamics induced by different microenvironments in nanoporous supports using a benchtop technique. As composites with faster PEI dynamics have been found to be more efficient for CO_2 capture, the results are also particularly relevant for carbon capture applications. We believe that understanding

https://doi.org/10.1021/acs.jpcc.2c01099
J. Phys. Chem. C 2022, 126, 10419−10428

how the aminopolymer mobility is influenced by nanoconfinement and other environmental factors and conditions will ultimately be critical to the development of more efficient DAC systems employing these materials, and we contend that this technique is a powerful means for advancing that understanding.

■ ASSOCIATED CONTENT

Supporting Information

The Supporting Information is available free of charge at https://pubs.acs.org/doi/10.1021/acs.jpcc.2c01099.

DSC traces, TGA data, nitrogen isotherms, emission spectra (PDF)

■ AUTHOR INFORMATION

Corresponding Author

Wade A. Braunecker − *Department of Chemistry, Colorado School of Mines, Golden, Colorado 80401, United States; National Renewable Energy Laboratory, Golden, Colorado 80401, United States;* orcid.org/0000-0003-0773-9580; Email: Wade.Braunecker@nrel.gov

Authors

Helen Correll − *Department of Chemistry, Colorado School of Mines, Golden, Colorado 80401, United States; National Renewable Energy Laboratory, Golden, Colorado 80401, United States*

Noemi Leick − *National Renewable Energy Laboratory, Golden, Colorado 80401, United States;* orcid.org/0000-0002-2014-6264

Rachel E. Mow − *Department of Chemistry, Colorado School of Mines, Golden, Colorado 80401, United States; National Renewable Energy Laboratory, Golden, Colorado 80401, United States*

Glory A. Russell-Parks − *Department of Chemistry, Colorado School of Mines, Golden, Colorado 80401, United States; National Renewable Energy Laboratory, Golden, Colorado 80401, United States;* orcid.org/0000-0001-9059-1681

Simon H. Pang − *Materials Science Division, Lawrence Livermore National Laboratory, Livermore, California 94550, United States;* orcid.org/0000-0003-2913-1648

Thomas Gennett − *Department of Chemistry, Colorado School of Mines, Golden, Colorado 80401, United States; National Renewable Energy Laboratory, Golden, Colorado 80401, United States*

Complete contact information is available at: https://pubs.acs.org/10.1021/acs.jpcc.2c01099

Notes

The authors declare no competing financial interest.

■ ACKNOWLEDGMENTS

This work was authored in part by Alliance for Sustainable Energy, LLC, the manager and operator of the National Renewable Energy Laboratory for the U.S. Department of Energy (DOE) under Contract No. DE-AC36-08GO28308. Work at the Lawrence Livermore National Laboratory was performed under the auspices of the U.S. DOE under Contract DE-AC52-07NA27344. This work was supported by the U.S. Department of Energy, Office of Science, Basic Energy Sciences, Materials Sciences and Engineering Division. The views expressed in the article do not necessarily represent the views of the DOE or the U.S. Government. The U.S. Government retains and the publisher, by accepting the article for publication, acknowledges that the U.S. Government retains a nonexclusive, paid-up, irrevocable, worldwide license to publish or reproduce the published form of this work, or allow others to do so, for U.S. Government purposes.

■ REFERENCES

(1) National Academies of Sciences, Engineering, and Medicine. *Negative Emissions Technologies and Reliable Sequestration: A Research Agenda*; The National Academies Press, 2019.

(2) Baker, S. E.; Stolaroff, J. K.; Peridas, G.; Pang, S. H.; Goldstein, H. M.; Lucci, F. R.; Li, W.; Slessarev, E. W.; Pett-Ridge, J.; Ryerson, F. J.et al.*Getting to Neutral: Options for Negative Carbon Emissions in California*, LLNL-TR-796100; Lawrence Livermore National Laboratory: Livermore, CA, 2020.

(3) Sanz-Pérez, E. S.; Murdock, C. R.; Didas, S. A.; Jones, C. W. Direct Capture of CO2 from Ambient Air. *Chem. Rev.* **2016**, *116*, 11840−11876.

(4) Beuttler, C.; Charles, L.; Wurzbacher, J. The Role of Direct Air Capture in Mitigation of Anthropogenic Greenhouse Gas Emissions. *Front. Clim.* **2019**, *1*, No. 10.

(5) Shi, X.; Xiao, H.; Azarabadi, H.; Song, J.; Wu, X.; Chen, X.; Lackner, K. S. Sorbents for the Direct Capture of CO2 from Ambient Air. *Angew. Chem., Int. Ed.* **2020**, *59*, 6984−7006.

(6) McQueen, N.; Gomes, K. V.; McCormick, C.; Blumanthal, K.; Pisciotta, M.; Wilcox, J. A review of direct air capture (DAC): scaling up commercial technologies and innovating for the future. *Prog. Energy* **2021**, *3*, No. 032001.

(7) Xu, X.; Song, C.; Andresen, J. M.; Miller, B. G.; Scaroni, A. W. Novel Polyethylenimine-Modified Mesoporous Molecular Sieve of MCM-41 Type as High-Capacity Adsorbent for CO2 Capture. *Energy Fuels* **2002**, *16*, 1463−1469.

(8) Son, W.-J.; Choi, J.-S.; Ahn, W.-S. Adsorptive removal of carbon dioxide using polyethyleneimine-loaded mesoporous silica materials. *Microporous Mesoporous Mater.* **2008**, *113*, 31−40.

(9) Goeppert, A.; Czaun, M.; May, R. B.; Prakash, G. K. S.; Olah, G. A.; Narayanan, S. R. Carbon Dioxide Capture from the Air Using a Polyamine Based Regenerable Solid Adsorbent. *J. Am. Chem. Soc.* **2011**, *133*, 20164−20167.

(10) Chaikittisilp, W.; Kim, H.-J.; Jones, C. W. Mesoporous Alumina-Supported Amines as Potential Steam-Stable Adsorbents for Capturing CO2 from Simulated Flue Gas and Ambient Air. *Energy Fuels* **2011**, *25*, 5528−5537.

(11) Sakwa-Novak, M. A.; Jones, C. W. Steam Induced Structural Changes of a Poly(ethylenimine) Impregnated γ-Alumina Sorbent for CO2 Extraction from Ambient Air. *ACS Appl. Mater. Interfaces* **2014**, *6*, 9245−9255.

(12) Goeppert, A.; Zhang, H.; Czaun, M.; May, R. B.; Prakash, G. K. S.; Olah, G. A.; Narayanan, S. R. Easily Regenerable Solid Adsorbents Based on Polyamines for Carbon Dioxide Capture from the Air. *ChemSusChem* **2014**, *7*, 1386−1397.

(13) Zhang, H.; Goeppert, A.; Prakash, G. K. S.; Olah, G. Applicability of linear polyethylenimine supported on nano-silica for the adsorption of CO2 from various sources including dry air. *RSC Adv.* **2015**, *5*, 52550−52562.

(14) Sakwa-Novak, M. A.; Yoo, C.-J.; Tan, S.; Rashidi, F.; Jones, C. W. Poly(ethylenimine)-Functionalized Monolithic Alumina Honeycomb Adsorbents for CO2 Capture from Air. *ChemSusChem* **2016**, *9*, 1859−1868.

(15) Sayari, A.; Liu, Q.; Mishra, P. Enhanced Adsorption Efficiency through Materials Design for Direct Air Capture over Supported Polyethylenimine. *ChemSusChem* **2016**, *9*, 2796−2803.

(16) Kwon, H. T.; Sakwa-Novak, M. A.; Pang, S. H.; Sujan, A. R.; Ping, E. W.; Jones, C. W. Aminopolymer-Impregnated Hierarchical Silica Structures: Unexpected Equivalent CO2 Uptake under Simulated Air Capture and Flue Gas Capture Conditions. *Chem. Mater.* **2019**, *31*, 5229−5237.

(17) Sujan, A. R.; Pang, S. H.; Zhu, G.; Jones, C. W.; Lively, R. P. Direct CO2 Capture from Air using Poly(ethylenimine)-Loaded Polymer/Silica Fiber Sorbents. *ACS Sustainable Chem. Eng.* **2019**, *7*, 5264−5273.
(18) Lively, R. P.; Realff, M. J. On thermodynamic separation efficiency: Adsorption processes. *AIChE J.* **2016**, *62*, 3699−3705.
(19) Robeson, L. M.; Liu, Q.; Freeman, B. D.; Paul, D. R. Comparison of transport properties of rubbery and glassy polymers and the relevance to the upper bound relationship. *J. Membr. Sci.* **2015**, *476*, 421−431.
(20) Sakwa-Novak, M. A.; Tan, S.; Jones, C. W. Role of Additives in Composite PEI/Oxide CO2 Adsorbents: Enhancement in the Amine Efficiency of Supported PEI by PEG in CO2 Capture from Simulated Ambient Air. *ACS Appl. Mater. Interfaces* **2015**, *7*, 24748−24759.
(21) Ellison, C. J.; Torkelson, J. M. The distribution of glass-transition temperatures in nanoscopically confined glass formers. *Nat. Mater.* **2003**, *2*, 695−700.
(22) Elmahdy, M. M.; Chrissopoulou, K.; Afratis, A.; Floudas, G.; Anastasiadis, S. H. Effect of Confinement on Polymer Segmental Motion and Ion Mobility in PEO/Layered Silicate Nanocomposites. *Macromolecules* **2006**, *39*, 5170−5173.
(23) Rittigstein, P.; Priestley, R. D.; Broadbelt, L. J.; Torkelson, J. M. Model polymer nanocomposites provide an understanding of confinement effects in real nanocomposites. *Nat. Mater.* **2007**, *6*, 278−282.
(24) Uemura, T.; Yanai, N.; Watanabe, S.; Tanaka, H.; Numaguchi, R.; Miyahara, M. T.; Ohta, Y.; Nagaoka, M.; Kitagawa, S. Unveiling thermal transitions of polymers in subnanometre pores. *Nat. Commun.* **2010**, *1*, No. 83.
(25) Stafford, C. M.; Harrison, C.; Beers, K. L.; Karim, A.; Amis, E. J.; VanLandingham, M. R.; Kim, H.-C.; Volksen, W.; Miller, R. D.; Simonyi, E. E. A buckling-based metrology for measuring the elastic moduli of polymeric thin films. *Nat. Mater.* **2004**, *3*, 545−550.
(26) Stafford, C. M.; Vogt, B. D.; Harrison, C.; Julthongpiput, D.; Huang, R. Elastic Moduli of Ultrathin Amorphous Polymer Films. *Macromolecules* **2006**, *39*, 5095−5099.
(27) O'Connell, P. A.; McKenna, G. B. The stiffening of ultrathin polymer films in the rubbery regime: The relative contributions of membrane stress and surface tension. *J. Polym. Sci., Part B: Polym. Phys.* **2009**, *47*, 2441−2448.
(28) Li, X.; McKenna, G. B. Ultrathin Polymer Films: Rubbery Stiffening, Fragility, and Tg Reduction. *Macromolecules* **2015**, *48*, 6329−6336.
(29) Mapesa, E. U.; Cantillo, N. M.; Hamilton, S. T.; Harris, M. A.; Zawodzinski, T. A.; Park, A.-H.; Sangoro, J. Localized and Collective Dynamics in Liquid-like Polyethylenimine-Based Nanoparticle Organic Hybrid Materials. *Macromolecules* **2021**, *54*, 2296−2305.
(30) Holewinski, A.; Sakwa-Novak, M. A.; Jones, C. W. Linking CO2 Sorption Performance to Polymer Morphology in Amino-polymer/Silica Composites through Neutron Scattering. *J. Am. Chem. Soc.* **2015**, *137*, 11749−11759.
(31) Holewinski, A.; Sakwa-Novak, M. A.; Carrillo, J. Y.; Potter, M. E.; Ellebracht, N.; Rother, G.; Sumpter, B. G.; Jones, C. W. Aminopolymer Mobility and Support Interactions in Silica-PEI Composites for CO2 Capture Applications: A Quasielastic Neutron Scattering Study. *J. Phys. Chem. B* **2017**, *121*, 6721−6731.
(32) Zhang, R.; Wang, X.; Liu, S.; He, L.; Song, C.; Jiang, X.; Blach, T. P. Discovering Inherent Characteristics of Polyethylenimine-Functionalized Porous Materials for CO2 Capture. *ACS Appl. Mater. Interfaces* **2019**, *11*, 36515−36524.
(33) Burroughs, M. J.; Christie, D.; Gray, L. A. G.; Chowdhury, M.; Priestley, R. D. 21st Century Advances in Fluorescence Techniques to Characterize Glass-Forming Polymers at the Nanoscale. *Macromol. Chem. Phys.* **2018**, *219*, No. 1700368.
(34) Hooker, J. C.; Torkelson, J. M. Coupling of Probe Reorientation Dynamics and Rotor Motions to Polymer Relaxation As Sensed by Second Harmonic Generation and Fluorescence. *Macromolecules* **1995**, *28*, 7683−7692.
(35) Bao, S.; Wu, Q.; Qin, W.; Yu, Q.; Wang, J.; Liang, G.; Tang, B. Z. Sensitive and reliable detection of glass transition of polymers by fluorescent probes based on AIE luminogens. *Polym. Chem.* **2015**, *6*, 3537−3542.
(36) Paeng, K.; Swallen, S. F.; Ediger, M. D. Direct Measurement of Molecular Motion in Freestanding Polystyrene Thin Films. *J. Am. Chem. Soc.* **2011**, *133*, 8444−8447.
(37) Paeng, K.; Richert, R.; Ediger, M. D. Molecular mobility in supported thin films of polystyrene, poly(methyl methacrylate), and poly(2-vinyl pyridine) probed by dye reorientation. *Soft Matter* **2012**, *8*, 819−826.
(38) Ellison, C. J.; Kim, S. D.; Hall, D. B.; Torkelson, J. M. Confinement and processing effects on glass transition temperature and physical aging in ultrathin polymer films: Novel fluorescence measurements. *Eur. Phys. J. E* **2002**, *8*, 155−166.
(39) Priestley, R. D.; Ellison, C. J.; Broadbelt, L. J.; Torkelson, J. M. Structural Relaxation of Polymer Glasses at Surfaces, Interfaces, and In Between. *Science* **2005**, *309*, 456−459.
(40) Askar, S.; Evans, C. M.; Torkelson, J. M. Residual stress relaxation and stiffness in spin-coated polymer films: Characterization by ellipsometry and fluorescence. *Polymer* **2015**, *76*, 113−122.
(41) Askar, S.; Torkelson, J. M. Stiffness of thin, supported polystyrene films: Free-surface, substrate, and confinement effects characterized via self-referencing fluorescence. *Polymer* **2016**, *99*, 417−426.
(42) Kim, S.; Torkelson, J. M. Distribution of Glass Transition Temperatures in Free-Standing, Nanoconfined Polystyrene Films: A Test of de Gennes' Sliding Motion Mechanism. *Macromolecules* **2011**, *44*, 4546−4553.
(43) Baglay, R. R.; Roth, C. B. Communication: Experimentally determined profile of local glass transition temperature across a glassy-rubbery polymer interface with a Tg difference of 80 K. *J. Chem. Phys.* **2015**, *143*, No. 111101.
(44) Baglay, R. R.; Roth, C. B. Local glass transition temperature Tg(z) of polystyrene next to different polymers: Hard vs. soft confinement. *J. Chem. Phys.* **2017**, *146*, No. 203307.
(45) Mundra, M. K.; Ellison, C. J.; Rittigstein, P.; Torkelson, J. M. Fluorescence studies of confinement in polymer films and nanocomposites: Glass transition temperature, plasticizer effects, and sensitivity to stress relaxation and local polarity. *Eur. Phys. J. Spec. Top.* **2007**, *141*, 143.
(46) Lu, W.; Xiao, P.; Gu, J.; Zhang, J.; Huang, Y.; Huang, Q.; Chen, T. Aggregation-induced emission of tetraphenylethylene-modified polyethyleneimine for highly selective CO2 detection. *Sens. Actuators, B* **2016**, *228*, 551−556.
(47) Wang, C.; Li, Q.; Wang, B.; Li, D.; Yu, J. Fluorescent sensors based on AIEgen-functionalised mesoporous silica nanoparticles for the detection of explosives and antibiotics. *Inorg. Chem. Front.* **2018**, *5*, 2183−2188.
(48) Potter, M. E.; Pang, S. H.; Jones, C. W. Adsorption Microcalorimetry of CO2 in Confined Aminopolymers. *Langmuir* **2017**, *33*, 117−124.
(49) Mei, J.; Leung, N. L. C.; Kwok, R. T. K.; Lam, J. W. Y.; Tang, B. Z. Aggregation-Induced Emission: Together We Shine, United We Soar! *Chem. Rev.* **2015**, *115*, 11718−11940.
(50) La, D. D.; Bhosale, S. V.; Jones, L. A.; Bhosale, S. V. Tetraphenylethylene-Based AIE-Active Probes for Sensing Applications. *ACS Appl. Mater. Interfaces* **2018**, *10*, 12189−12216.
(51) Sharath Kumar, K. S.; Girish, Y. R.; Ashrafizadeh, M.; Mirzaei, S.; Rakesh, K. P.; Hossein Gholami, M.; Zabolian, A.; Hushmandi, K.; Orive, G.; Kadumudi, F. B.; Dolatshahi-Pirouz, A.; Thakur, V. K.; Zarrabi, A.; Makvandi, P.; Rangappa, K. S. AIE-featured tetraphenylethylene nanoarchitectures in biomedical application: Bioimaging, drug delivery and disease treatment. *Coord. Chem. Rev.* **2021**, *447*, No. 214135.
(52) Yang, Z.; Chi, Z.; Mao, Z.; Zhang, Y.; Liu, S.; Zhao, J.; Aldred, M. P.; Chi, Z. Recent advances in mechano-responsive luminescence of tetraphenylethylene derivatives with aggregation-induced emission properties. *Mater. Chem. Front.* **2018**, *2*, 861−890.

https://doi.org/10.1021/acs.jpcc.2c01099
J. Phys. Chem. C 2022, 126, 10419−10428

(53) Iasilli, G.; Battisti, A.; Tantussi, F.; Fuso, F.; Allegrini, M.; Ruggeri, G.; Pucci, A. Aggregation-Induced Emission of Tetraphenylethylene in Styrene-Based Polymers. *Macromol. Chem. Phys.* **2014**, *215*, 499−506.
(54) Barbara, P. F.; Rand, S. D.; Rentzepis, P. M. Direct measurements of tetraphenylethylene torsional motion by picosecond spectroscopy. *J. Am. Chem. Soc.* **1981**, *103*, 2156−2162.
(55) Demchenko, A. P. The concept of λ-ratiometry in fluorescence sensing and imaging. *J. Fluoresc.* **2010**, *20*, 1099−1128.
(56) Jimbo, T.; Tsuji, M.; Taniguchi, R.; Sada, K.; Kokado, K. Control of Aggregation-Induced Emission from a Tetraphenylethene Derivative through the Components in the Co-crystal. *Cryst. Growth Des.* **2018**, *18*, 3863−3869.
(57) Román, F.; Colomer, P.; Calventus, Y.; Hutchinson, J. M. Study of Hyperbranched Poly(ethyleneimine) Polymers of Different Molecular Weight and Their Interaction with Epoxy Resin. *Materials* **2018**, *11*, No. 410.
(58) Hashida, T.; Tashiro, K. Structural Study on Water-induced Phase Transitions of Poly(ethylene imine) as Viewed from the Simultaneous Measurements of Wide-Angle X-ray Diffractions and DSC Thermograms. *Macromol. Symp.* **2006**, *242*, 262−267.
(59) Aldred, M. P.; Li, C.; Zhu, M.-Q. Optical Properties and Photo-Oxidation of Tetraphenylethene-Based Fluorophores. *Chem.—Eur. J.* **2012**, *18*, 16037−16045.
(60) Badrinarayanan, P.; Zheng, W.; Li, Q.; Simon, S. L. The glass transition temperature versus the fictive temperature. *J. Non-Cryst. Solids* **2007**, *353*, 2603−2612.
(61) Plazek, D. J.; Ngai, K. L. The Glass Temperature. In *Physical Properties of Polymers Handbook*, 2nd; Mark, J. E., Ed.; Springer Nature, 2007; pp 187−215.
(62) McKenna, G. B.; Simon, S. L. 50th Anniversary Perspective: Challenges in the Dynamics and Kinetics of Glass-Forming Polymers. *Macromolecules* **2017**, *50*, 6333−6361.
(63) McKenna, G. B. Diverging views on glass transition. *Nat. Phys.* **2008**, *4*, 673.
(64) Plazek, D. J.; Frund, Z. N., Jr. Epoxy resins (DGEBA): The curing and physical aging process. *J. Polym. Sci., Part B: Polym. Phys.* **1990**, *28*, 431−448.
(65) Kunal, K.; Robertson, C. G.; Pawlus, S.; Hahn, S. F.; Sokolov, A. P. Role of Chemical Structure in Fragility of Polymers: A Qualitative Picture. *Macromolecules* **2008**, *41*, 7232−7238.
(66) Fried, J. R. Sub Tg Transitions. In *Physical Properties of Polymers Handbook*, 2nd ed.; Mark, J. E., Ed.; Springer Nature, 2007; pp 217−232.
(67) Hill, A. J.; Tant, M. R. The Structure and Properties of Glassy Polymers. *Structure and Properties of Glassy Polymers*, American Chemical Society, 1999; pp 1−20.
(68) Toi, K.; Ito, T.; Ikemoto, I. Effect of aging and conditioning on the gas transport of poly(vinyl acetate). *J. Polym. Sci., Polym. Lett. Ed.* **1985**, *23*, 525−529.
(69) Chowdhury, M.; Priestley, R. D. Discrete mobility on the surface of glasses. *Proc. Natl. Acad. Sci. U.S.A.* **2017**, *114*, 4854−4856.
(70) Kim, H.; Cang, Y.; Kang, E.; Graczykowski, B.; Secchi, M.; Montagna, M.; Priestley, R. D.; Furst, E. M.; Fytas, G. Direct observation of polymer surface mobility via nanoparticle vibrations. *Nat. Commun.* **2018**, *9*, No. 2918.
(71) Zhang, W.; Douglas, J. F.; Starr, F. W. Why we need to look beyond the glass transition temperature to characterize the dynamics of thin supported polymer films. *Proc. Nat. Acad. Sci. U.S.A.* **2018**, *115*, 5641−5646.

https://doi.org/10.1021/acs.jpcc.2c01099
J. Phys. Chem. C 2022, 126, 10419−10428